Organic & Biomolecular Chemistry

ROYAL SOCIETY OF CHEMISTRY

PAPER

View Article Online
View Journal | View Issue

Cite this: *Org. Biomol. Chem.*, 2026, **24**, 873

High-throughput DoE synthesis of chalcones and pyrazolines for fluorescent sensing

Alexander Ciupa

Received 26th October 2025,
Accepted 22nd December 2025

DOI: 10.1039/d5ob01684c

rsc.li/obc

Pyrazolines are attractive scaffolds for fluorescent sensors due to their unique photophysical properties and the ease of their synthesis from chalcone precursors. While both chalcones and pyrazolines have been widely explored, a systematic optimization of their synthesis using design of experiments (DoE) has yet to be reported. Here, we apply a data-driven DoE strategy, evaluating multiple variables across more than 105 datapoints, to establish highly optimized conditions for the Claisen–Schmidt condensation of chalcones and their subsequent conversion to pyrazolines. High-throughput screening of the resulting library revealed pyrazoline **P10** with unusual "turn on" fluorescence at 590 nm in the presence of Zn^{2+} only. This integrated DoE–HTS workflow demonstrates a powerful approach for accelerating sensor discovery.

Introduction

The integration of modern data-driven methodology into synthetic organic chemistry is streamlining synthetic method development.[1] Among these, design of experiments (DoE) enables the systematic identification of optimal parameters with a minimal number of experiments, offering a powerful alternative to the traditional one-factor-at-a-time (OFAT) strategy.[2] For instance, recent examples include the use of DoE in Heck–Suzuki reactions,[3] $B(OCH_2CF_3)_3$-mediated direct amidation,[4] and solvent selection for multicomponent reactions.[5] In parallel, high-throughput screening (HTS) platforms are accelerating the discovery process, with improvements reported in drug development,[6] enhanced catalyst screening,[7] and solar cell optimisation.[8] Both DoE and HTS approaches benefit from modular, easily accessible chemical scaffolds. Chalcones are privileged structures[9] with a diverse range of pharmacological properties, including anti-cancer,[10] anti-inflammatory,[11] and anti-infective properties.[12] Typically, chalcones are prepared *via* a Claisen–Schmidt condensation[13] from commercially available aromatic ketone and aldehyde starting materials (Fig. 1A). The diverse range of inexpensive, commercially available starting materials enables large modular libraries of chalcones to be synthesized and screened. Interest in Claisen–Schmidt condensations has grown considerably over the past sixty years (Fig. 1B). Importantly, while useful in themselves, chalcones can also serve as valuable precursors for pyrazolines (blue in Fig. 1A), another privileged structure with multiple medicinal properties.[14] Pyrazolines with nanomolar activities for cancer cell lines[15] and COX inhibitory activity have been reported.[16] Pyrazolines can be aromatised to pyrazoles[17] (red in Fig. 1A), providing access to another highly attractive privileged structure.[18] Despite the wealth of applications chalcones and pyrazolines provide, no DoE study has optimised access to these scaffolds. This study addresses this research gap, providing efficient access to chalcone and pyra-

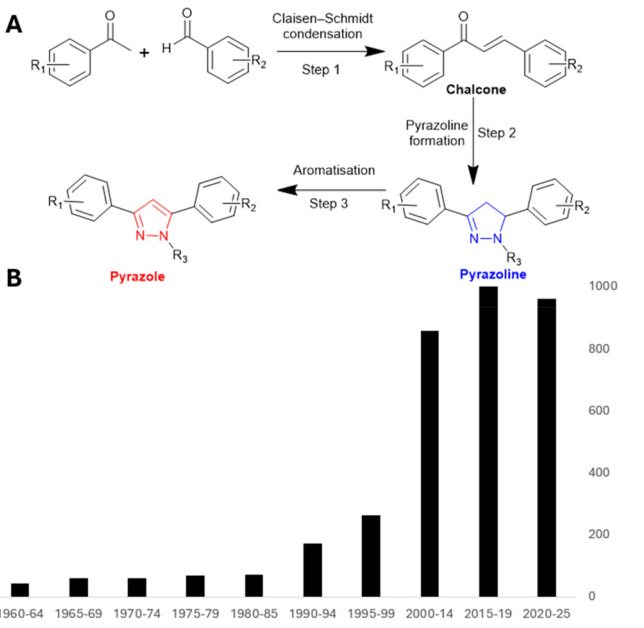

Fig. 1 Access to pyrazoline and pyrazoles *via* the chalcone scaffold (panel A). Claisen–Schmidt condensations reported between 1960 and 2025 *via* the Reaxys database (panel B).

Materials Innovation Factory, University of Liverpool, 51 Oxford Street, Liverpool L7 3NY, UK. E-mail: ciupa@liverpool.ac.uk

zolines *via* DoE while exploring HTS platforms in pursuit of novel fluorescent sensors.

Pyrazolines display unique fluorescence properties for the design of fluorescent sensors for toxic metals such as Zn^{2+}, Cu^{2+}, and Hg^{2+}.[19] The modular nature of the pyrazolines scaffold enables fine-tuning of photophysical properties, a useful feature for sensor development. The use of pyrazoline[20] and pyrazole[21] sensors for detecting toxic metals in biological environments represents a growing area of interest. Group 12 sensors, which selectively detect and distinguish Zn^{2+}, Cd^{2+}, and Hg^{2+}, are particularly challenging. Zinc, the second most abundant transition metal in the human body, is vital for life,[22] cadmium is highly toxic and linked to numerous cancers,[23] and mercury displays potent neurotoxicity.[24] Few fluorescent sensors can differentiate between these metals at different fluorescence wavelengths (λ_{em}).[25] Simple pyrazoline **A** is a highly selective "turn on" sensor for Zn^{2+} and Cd^{2+} in MeCN (Fig. 2).[26] Further studies revealed pyrazole **B** with improved selectivity for Zn^{2+}/Cd^{2+} (Fig. 2).[27] Pyrazoline **C** is a "turn on" sensor for Fe^{3+}/Fe^{2+} with yellow λ_{em}.[28] Substitution of the pyrazoline N1 methyl for phenyl reversed the fluorescent response from "turn on" to "turn off" (**D** in Fig. 2).[28] The hydrazone functional group is commonly incorporated into multi-analyte fluorescent sensors.[29] A recent breakthrough reported first-in-class hydrazone-pyrazolines sensors distinguishing Zn^{2+} at 560 nm, Cd^{2+} at 510 nm, and Hg^{2+} at 460 nm λ_{em} in aqueous environments (**E** in Fig. 2).[30] Typical approaches to chalcones involve the use of polar protic solvents, such as ethanol and methanol, accounting for 50% and 20% of all Claisen–Schmidt condensations reported between 1960–2025 (see SI1 for literature survey). Researchers often use previous synthetic methodologies with little to no experimental optimisation reported. This study addresses this research need using a data-driven design of experiments (DoE) approach. A large-scale chalcone library (>1 g scale) enabled a second DoE study focusing on pyrazoline synthesis. A pyrazoline library was generated, screened across multiple analytes using a HTS platform. This workflow significantly accelerated the discovery process, providing a valuable case study on incorporating data-driven methodology in synthetic organic chemistry.

Results and discussion

An LC-MS method to monitor the Claisen–Schmidt condensation reaction was established (Fig. 3). An internal standard (acetaminophen) was added to all reaction aliquots ensuring injection consistency, and external calibration curves were generated (see SI3 for full details). A typical chromatogram is displayed in Fig. 3 demonstrating the conversion of 2-acetylpyridine and benzaldehyde to **C1**. A screening study to confirm the suitability of the LC-MS method and determine the main DoE parameters was performed (SI4). Solvent, consisting of the bulk of the reaction mixture, had a significant impact on chalcone yield. The equivalent of NaOH, temperature, and time were also identified as significant factors and selected for DoE analysis. While this one factor at a time (OFAT) approach identified suitable conditions, it did not identify interconnected variables or provide a system-wide analysis. A DoE workflow was established (Fig. 4) to screen multiple variables; each performed in triplicate. This experimental design provided 45 datapoints to determine the optimum conditions for the Claisen–Schmidt condensation reaction[13] for chalcone synthesis using a system-wide approach.

A least squares fit DoE model was generated with an R^2 value of 0.97 and a P-value of <0.001, indicating good statistical modelling (Fig. 5C). This model was then used to predict various reaction conditions (Fig. 5A). Solvent was confirmed as influencing the reaction yield, with the polar protic solvents MeOH, EtOH, and IPA providing the best yields. Polar aprotic

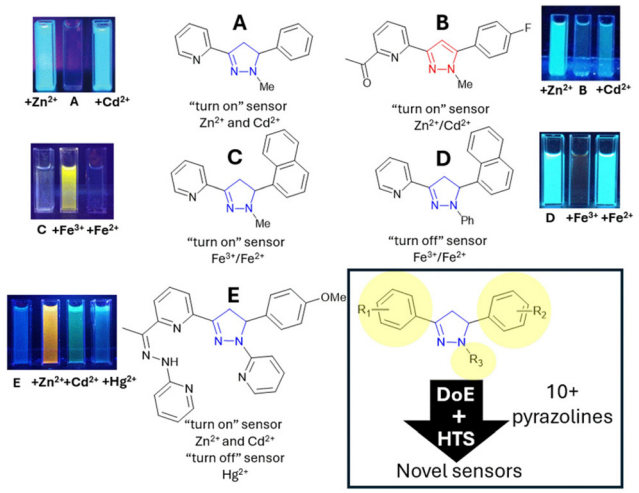

Fig. 2 Fluorescent sensors for toxic metals. This study incorporated design of experiments (DoE) and high throughput screening (HTS) for pyrazoline sensor development (inset).

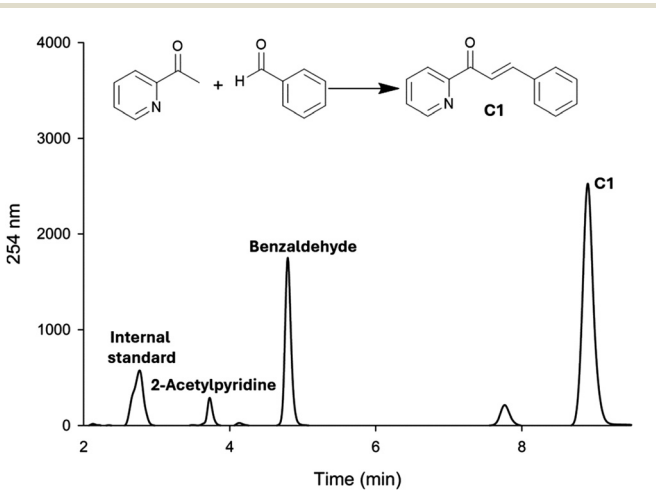

Fig. 3 Claisen–Schmidt condensation for **C1** monitored *via* LC-MS, starting materials 2-acetylpyridine and benzaldehyde to chalcone **C1** with acetaminophen used as an internal standard.

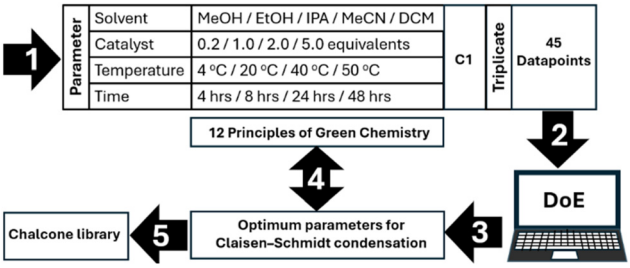

Fig. 4 DoE workflow for optimum chalcone synthesis using 45 individual datapoints.

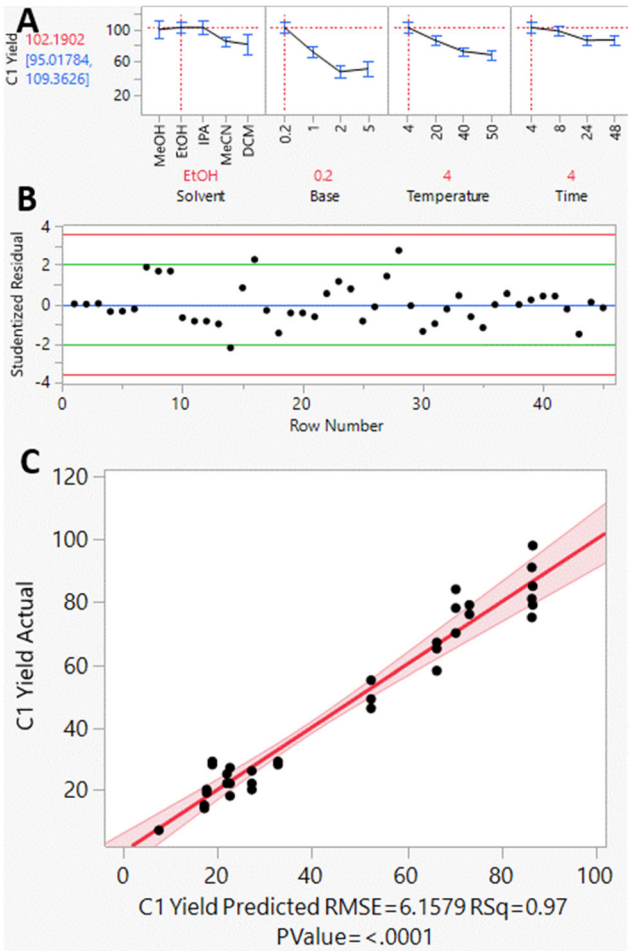

Fig. 5 DoE summary, optimal parameters are displayed in red (panel A), residuals in panel B. An excellent predictive model (R^2 = 0.97) was generated with confidence interval displayed in red (panel C).

solvent MeCN and chlorinated solvent dichloromethane should be avoided. Interestingly, the use of 0.2 equivalent NaOH was the most efficient alongside 4 °C reaction temperature. Further increases in catalyst and temperature were detrimental to reaction yield. Time had a minor influence on reaction yield, with 4 h and 8 h the optimal. Using the above model and the 12 principles of green chemistry,[31] particularly atom economy and energy efficiency, the following conditions were selected: EtOH, 0.2 equiv. NaOH, 4 °C and 8 h. These reaction conditions were then used to synthesise a structurally diverse library of 27 chalcones in excellent yield. Performing these reactions on a 10 mmol scale enabled gram-scale purification of chalcones directly *via* recrystallization preventing the requirement for time-consuming column chromatography (Scheme 1).

The high yield for chalcones **C1–C27** provides further confirmation of the predictive properties of the DoE model and validates the chosen reaction conditions (Table 1). These reaction conditions are likely to be suitable for future chalcone research beyond sensing, for example medicinal chemistry.[9–12] These chalcones then served as precursors for a pyrazoline synthesis DoE and, in turn, a pyrazoline library. A suitable DoE

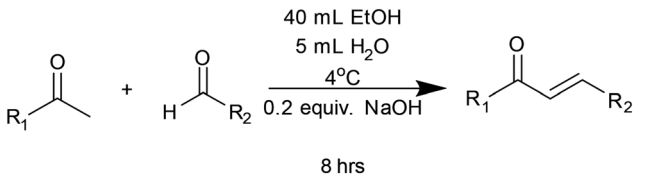

Scheme 1 DoE optimised chalcone synthesis.

Table 1 Chalcone library using DoE derived conditions

R1 / R2			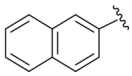
	**C1** 83%	**C10** 72%	**C19** 72%
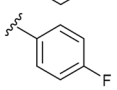	**C2** 72%	**C11** 73%	**C20** 76%
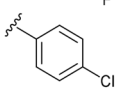	**C3** 86%	**C12** 77%	**C21** 79%
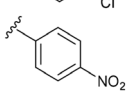	**C4** 60%	**C13** 84%	**C22** 72%
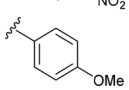	**C5** 75%	**C14** 60%	**C23** 70%
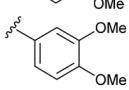	**C6** 89%	**C15** 65%	**C24** 89%
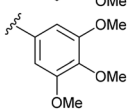	**C7** 87%	**C16** 74%	**C25** 95%
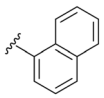	**C8** 92%	**C17** 84%	**C26** 76%
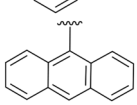	**C9** 77%	**C18** 73%	**C27** 75%

approach was developed to determine the optimal reaction conditions for the conversion of chalcone **C1** to pyrazoline **P1**. The same LC-MS method was utilized to monitor the conversion of **C1** to **P1** with a DoE workflow established to screen solvent, phenylhydrazine equivalent, temperature, and time (Fig. 6).

A least squares fit DoE model was generated with EtOH identified as the optimal medium for the reaction (Fig. 7).

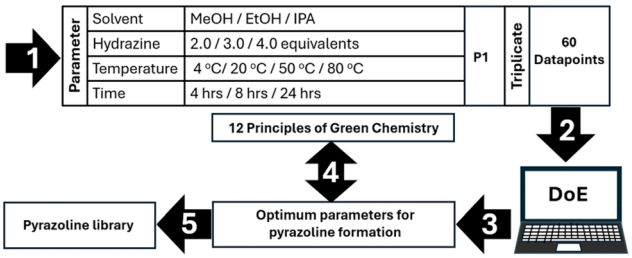

Fig. 6 DoE workflow for optimum pyrazoline synthesis using 60 individual datapoints.

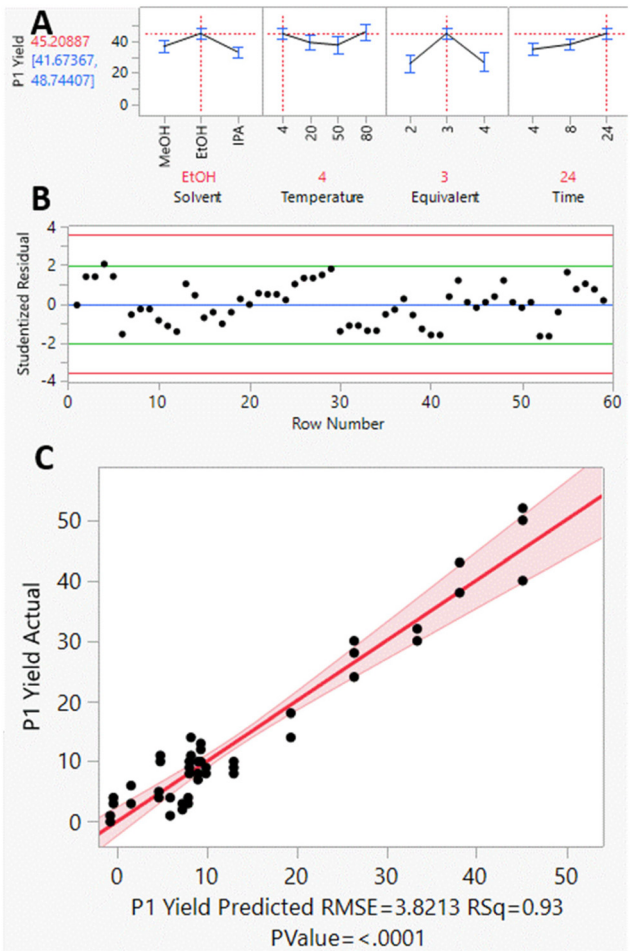

Fig. 7 DoE summary, optimal parameters are displayed in red (panel A), residuals in panel B. A good predictive model (R^2 = 0.93) was generated with confidence interval displayed in red (panel C).

Interestingly, temperature exerted only a minor influence on pyrazoline formation, with 4 °C providing the best outcome when used in combination with 3.0 equivalents of hydrazine.

Reaction time showed a linear correlation with product yield, and 24 hours was determined to be optimal. Guided by this optimization model and the 12 Principles of Green Chemistry,[31] the final reaction conditions were selected as EtOH, 3.0 equiv. hydrazine, 4 °C, and 24 h (Scheme 2). Under these conditions, a structurally diverse pyrazoline library comprising 11 potential sensors was synthesized in good to excellent yields (Fig. 8). Reactions performed on a 2 mmol scale generated sufficient material for purification *via* recrystallization, eliminating the need for time-consuming column chromatography. This approach was essential for achieving rapid synthesis and enabling high-throughput screening for desirable sensing properties. A preliminary fluorescence screen was performed to identify promising sensors in the presence of Zn^{2+} and Cd^{2+} (Fig. 8). Pyrazoline **P1–P3**, all containing a phenyl-substituted pyrazoline, displayed negligible changes in fluorescence emission with Zn^{2+} and Cd^{2+}. Interestingly, the pyridine-substituted analogues **P7–P9** did display a slight preference for Zn^{2+} over Cd^{2+} with green fluorescence emission. This observation suggested that the addition of nitrogen may be beneficial to group 12 metal selectivity. Pyrazoline **P11** displayed a "turn off" response, indicating the naphthyl unit is impacting the fluorescence response. The lead sensor was identified as **P10**, displaying both a nitro-substituted ring and pyridyl units. A highly unusual yellow fluorescence emission was observed in the presence of Zn^{2+}, but not with Cd^{2+}. The substitution of an electronegative halogen (as observed in **P8** and **P9**) for a highly electronegative nitro group profoundly modified the response to Zn^{2+} and Cd^{2+} and warrants further investigation. With a library of 11 pyrazolines in hand, a high-throughput screening (HTS) assay was developed using a standard laboratory fluorescence plate reader using a 96-well format. The responses to eleven different metal ions (250 μM) across each pyrazoline (50 μM) were measured in duplicate in acetonitrile.

This approach was designed to rapidly screen for fluorescence sensing properties in the 380–650 nm range using 360 nm excitation (see SI for full analysis, see Fig. 9 for heatmap summary). Pyrazoline **P1**, **P3–5**, **P7–P8**, and **P10** all displayed a "turn on" response to a range of group 12 metals. The paramagnetic metals Fe^{3+}, Ru^{3+}, and Cu^{2+} displayed a "turn off" response across all pyrazolines; this is commonly observed in the literature.[32] The biological metals Na^{+}, Li^{+}, and Mg^{2+} did not alter the fluorescence response, and therefore these sensors are unsuitable for monitoring these ana-

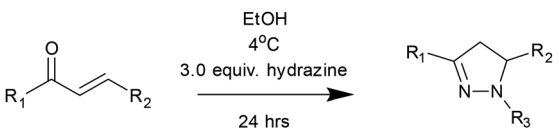

Scheme 2 DoE optimised pyrazoline synthesis.

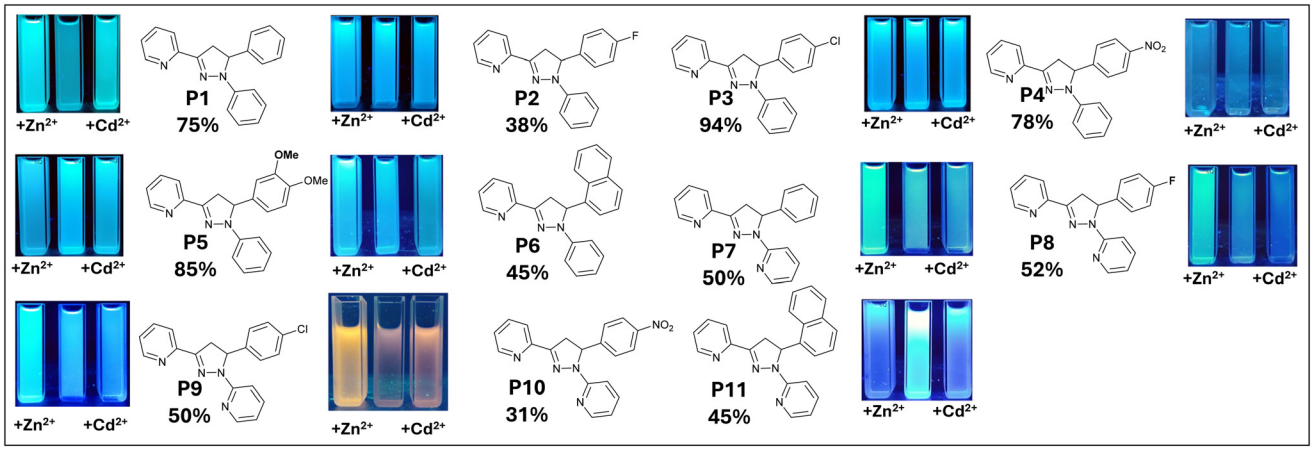

Fig. 8 Pyrazoline library with initial Zn^{2+} and Cd^{2+} screening using a 100 W 365 nm lamp.

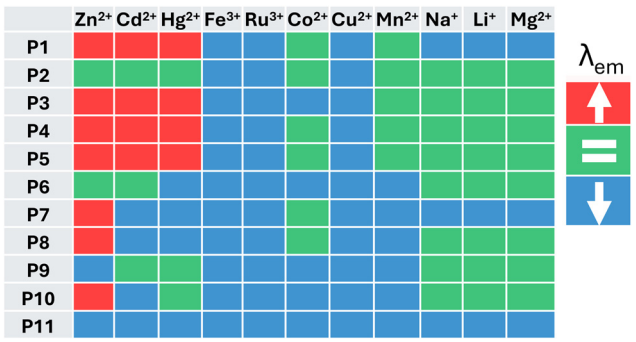

Fig. 9 High-throughput screening (HTS) of pyrazoline **P1–P11** using a fluorescence plate reader, λ_{ex} 360 nm, each result is average spectra from duplicate measurements. Colour indicates change in fluorescence, red represents an increase, blue a decrease and green no change in λ_{em}.

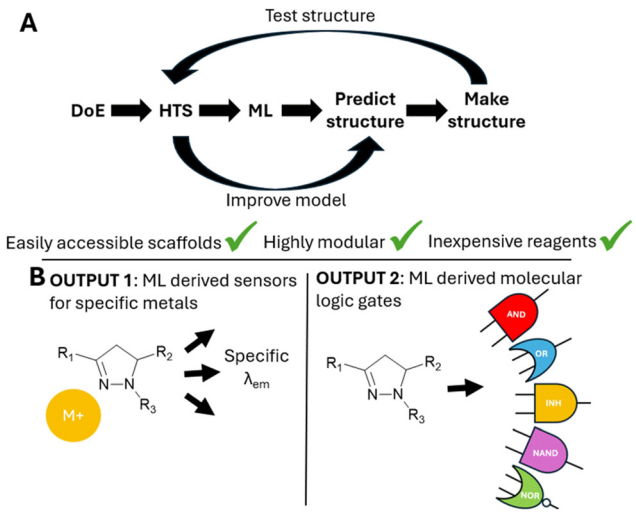

Fig. 11 Future workflow incorporating design of experiments (DoE), high-throughput screen (HTS), and machine learning (ML) to accelerate the discovery process (panel A). Potential outputs include ML-derived sensors for specific metals and the discovery of pyrazoline-based molecular logic gates (panel B).

lytes. The metal screen for **P10** is of particular interest as there is a "turn on" response only for Zn^{2+}, not Cd^{2+} or Hg^{2+}. The Stokes shift for **P10** is also unusually large, >240 nm and this is advantageous for sensing applications. This suggests **P10** could be a highly useful Zn^{2+} specific sensor and will be explored in future work. In summary, a combined DoE and HTS workflow has been established to rapidly synthesise a pyrazoline library from chalcone precursors in high yield. These sensors were rapidly screened for desirable sensing properties, resulting in the unexpected discovery of sensor **P10** with future potential.

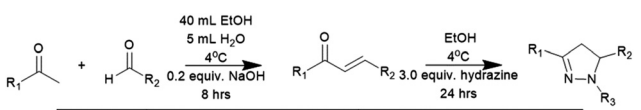

Parameter	Chalcone	Pyrazoline
Solvent	MeOH / **EtOH** / IPA / MeCN / DCM	MeOH / **EtOH** / IPA
Reagent	**0.2** / 1.0 / 2.0 / 5.0 equivalents	2.0 / **3.0** / 4.0 equivalents
Temperature	**4 °C** / 20 °C / 40 °C / 50 °C	**4 °C**/ 20 °C / 50 °C / 80 °C
Time	4 hrs / **8 hrs** / 24 hrs / 48 hrs	4 hrs / 8 hrs / **24 hrs**

Fig. 10 All DoE factors evaluated, with the best conditions in bold.

Conclusion

The optimised synthetic conditions for chalcone and pyrazoline formation has been determined using a data-driven design of experiments (DoE) approach (Fig. 10). These conditions (EtOH, 0.2 equiv. NaOH, 4 °C and 8 h) provided a diverse chalcone library of 27 compounds in good to excellent yield (60–93%, Table 1). The optimal conditions for pyrazoline formation (EtOH, 3.0 equiv. hydrazine, 4 °C, and 24 h) were determined and used to generate a pyrazoline library also in good to excellent yield (11–94%, Fig. 8).

The establishment of an HTS assay enabled the rapid identification of fluorescent properties to a range of metals, resulting in the highly expected discovery of **P10** with highly unusual yellow fluorescent emission in the presence of Zn^{2+}

only. This workflow demonstrates the significant advantages of incorporating modern data-driven methodology into synthetic organic chemistry. This approach is ideally suited to machine learning (ML) applications in which a large, structurally diverse, and modular chemical library is synthesized and screened, resulting in large datasets of consistent data.[33] This dataset can then be used to train ML models to predict and design novel compounds with specific properties (Fig. 11A). These, in turn, are generated and screened, and the resulting data used to improve the model further. A key requirement for this strategy is easily accessible scaffolds that are highly modular, using inexpensive reagents. As highlighted within, pyrazolines are ideally suited to this approach. Potential applications of such workflows include the generation of ML-derived sensors for specific metals and the development of molecular logic gates (Fig. 10B).[34] Numerous recent pyrazolines have been reported as logic gates,[35] and the application of ML will accelerate development further. This is future work and will be reported in due course.

Author contributions

Alexander Ciupa designed, synthesized, characterised all compounds, and authored the manuscript.

Conflicts of interest

There are no conflicts to declare.

Data availability

The data supporting this article have been included as part of the supplementary information (SI). Supplementary information is available. See DOI: https://doi.org/10.1039/d5ob01684c.

Acknowledgements

Krzysztof Pawlak is acknowledged for assistance with development of the high throughput screening assay and Steven Robinson for assistance with time-of-flight high resolution mass spectrometry. This work made use of shared equipment located at the Materials Innovation Factory, created as part of the UK Research Partnership Innovation Fund (Research England) and co-funded by the Sir Henry Royce Institute.

References

1 Selected examples: (*a*) A. F. de Almeida, R. Moreira and T. Rodrigues, *Nat. Rev. Chem.*, 2019, **3**, 589; (*b*) L. Himanen, A. Geurts, A. S. Foster and P. Rinke, *Adv. Sci.*, 2019, **6**, 1900808; (*c*) J. Y. Peng, D. Schwalbe-Koda, K. Akkiraju, T. Xie, L. Giordano, Y. Yu, C. J. Eom, J. R. Lunger, D. J. Zheng, R. R. Rao, S. Muy, J. C. Grossman, K. Reuter, R. Gómez-Bombarelli and Y. Shao-Horn, *Nat. Rev. Mater.*, 2022, **7**, 991.
2 K. Telford, *Johns Hopkins APL Tech. Dig.*, 2007, **27**, 224.
3 A. Ekebergh, C. Lingblom, P. Sandin, C. Wennerås and J. Mårtensson, *Org. Biomol. Chem.*, 2015, **13**, 3382.
4 V. Karaluka, R. M. Lanigan, P. M. Murray, M. Badland and T. D. Sheppard, *Org. Biomol. Chem.*, 2015, **13**, 10888.
5 P. M. Murray, F. Bellany, L. Benhamou, D.-K. Bučar, A. B. Tabor and T. D. Sheppard, *Org. Biomol. Chem.*, 2016, **14**, 2373.
6 J. R. Broach and J. Thorner, *Nature*, 1996, **384**, 14.
7 S. M. Senkan, *Nature*, 1998, **394**, 350.
8 X. Rodríguez-Martínez, E. Pascual-San-José and M. Campoy-Quiles, *Energy Environ. Sci.*, 2021, **14**, 3301.
9 P. Singh, A. Anand and V. Kumar, *Eur. J. Med. Chem.*, 2014, **85**, 758.
10 Selected examples: (*a*) C. Karthikeyan, N. S. H. Narayana Moorthy, S. Ramasamy, U. Vanam, E. Manivannan, D. Karunagaran and P. Trivedi, *Recent Pat. Anti-Cancer Drug Discovery*, 2015, **10**, 97; (*b*) S. Ducki, R. Forrest, J. A. Hadfield, A. Kendall, N. J. Lawrence, A. T. McGown and D. Rennison, *Bioorg. Med. Chem. Lett.*, 1998, **8**, 1051; (*c*) A. Ciupa, N. J. Griffiths, S. K. Light, P. J. Wood and L. Caggiano, *Med. Chem. Commun.*, 2011, **2**, 1011.
11 Selected examples: (*a*) Z. Nowakowska, *Eur. J. Med. Chem.*, 2007, **42**, 125; (*b*) A. Yadav, V. Sharma and G. Singh, *ChemistrySelect*, 2024, **9**, e202401321.
12 D. K. Mahapatra, S. K. Bharti and V. Asati, *Eur. J. Med. Chem.*, 2015, **101**, 496.
13 Selected examples: (*a*) L. Claisen and A. Claparède, *Ber. Dtsch. Chem. Ges.*, 1881, **14**, 2460; (*b*) J. G. Schmidt, *Ber. Dtsch. Chem. Ges.*, 1881, **14**, 1459; (*c*) D. Coutinho, H. G. Machado, V. H. Carvalho-Silva and W. A. da Silva, *Phys. Chem. Chem. Phys.*, 2021, **23**, 6738; (*d*) C. L. Perrin and J. Woo, *Phys. Chem. Chem. Phys.*, 2022, **24**, 18978.
14 B. Varghese, S. N. Al-Busafi, F. O. Suliman and S. M. Z. Al-Kindy, *RSC Adv.*, 2017, **7**, 46999.
15 D. Matiadis and M. Sagnou, *Int. J. Mol. Sci.*, 2020, **21**, 5507.
16 M. Mantzanidou, E. Pontiki and D. Hadjipavlou-Litina, *Molecules*, 2021, **26**, 3439.
17 Selected examples: (*a*) S. Hofmann, M. Linden, J. Neuner, F. N. Weber and S. R. Waldvogel, *Org. Biomol. Chem.*, 2023, **21**, 4694; (*b*) S. V. Gamapwar, N. P. Tale and N. N. Karade, *Synth. Commun.*, 2012, **42**, 2617; (*c*) A. Ciupa, *New J. Chem.*, 2024, **48**, 13900.
18 Selected examples: (*a*) M. A. Alam, *Future Med. Chem.*, 2023, **15**, 2011; (*b*) T. Sarwar, G. Mustafa, W. Zafar, A. U. Hassan, S. H. Sumrra and A. Asif, *J. Mol. Struct.*, 2025, **1348**, 143523.
19 Selected examples: (*a*) M. Z. Alam, S. Ahmad and S. A. Khan, *J. Fluoresc.*, 2025, **35**, 1241; (*b*) M. Mohasin and S. A. Khan, *J. Fluoresc.*, 2025, **35**, 2553; (*c*) M. Z. Alam, M. Mohasin, S. Ahmad, U. Salma and S. A. Khan, *J. Coord. Chem.*, 2025, **78**, 367.

20 Selected examples: (*a*) Z. Zhang, F. W. Wang, S. Q. Wang, F. Ge, B. X. Zhao and J. Y. Miao, *Org. Biomol. Chem.*, 2012, **10**, 8640; (*b*) R. Manjunath and P. Kannan, *New J. Chem.*, 2018, **42**, 10891; (*c*) Y. S. Yang, F. N. Wang, Y. P. Zhang, F. Yang and J. J. Xue, *J. Fluoresc.*, 2024, **34**, 159; (*d*) Y. P. Zhang, Y. Y. Dong, Y. S. Yang, H. C. Guo, B. X. Cao and S. Q. Sun, *Spectrochim. Acta, Part A*, 2017, **177**, 147; (*e*) T. T. Zhang, F. W. Wang, M. M. Li, J. T. Liu, J. Y. Miao and B. X. Zhao, *Sens. Actuators, B*, 2013, **186**, 755.

21 Selected examples: (*a*) S. Gond, P. Yadav, A. Singh, S. Garai, A. Shekher, S. C. Gupta and V. P. Singh, *Org. Biomol. Chem.*, 2023, **21**, 4482; (*b*) A. Tigreros and J. Portilla, *Curr. Chin. Sci.*, 2021, **1**, 197; (*c*) S. Saha, A. De, A. Ghosh, A. Ghosh, K. Bera, K. S. Das, S. Akhtar, N. C. Maiti, A. K. Das, B. B. Das and R. Mondal, *RSC Adv.*, 2021, **11**, 10094; (*d*) A. Dhara, N. Guchhait, I. Mukherjee, A. Mukherjee and S. Chandra Bhattacharya, *RSC Adv.*, 2016, **6**, 105930.

22 C. T. Chasapis, C. A. Spiliopoulou, A. C. Loutsidou and M. E. Stefanidou, *Arch. Toxicol.*, 2012, **86**, 521.

23 G. Genchi, S. M. Sinicropi, G. Lauria, A. Carocci and A. Catalano, *Int. J. Environ. Res. Public Health*, 2020, **17**, 3782.

24 Y. S. Wu, A. I. Osman, M. Hosny, A. M. Elgarahy, A. S. Eltaweil, D. W. Rooney, Z. Chen, N. S. Rahim, M. Sekar, S. C. B. Gopinath, N. N. Mat Rani, K. Batumalaie and P. S. Yap, *ACS Omega*, 2024, **9**, 5100.

25 Selected examples: (*a*) Z. Xu, K.-H. Baek, H. N. Kim, J. Cui, X. Qian, D. R. Spring, I. Shin and J. Yoon, *J. Am. Chem. Soc.*, 2010, **132**, 601; (*b*) Y. Tan, J. Gao, J. Yu, Z. Wang, Y. Cui, Y. Yang and G. Qian, *Dalton Trans.*, 2013, **42**, 11465; (*c*) G. Tian, Y.-Z. Han and Q. Yang, *J. Mol. Struct.*, 2023, **1273**, 134341.

26 A. Ciupa, M. F. Mahon, P. A. De Bank and L. Caggiano, *Org. Biomol. Chem.*, 2012, **10**, 8753.

27 A. Ciupa, *RSC Adv.*, 2024, **14**, 3519.

28 A. Ciupa, *RSC Adv.*, 2024, **14**, 34918.

29 A. Ciupa, *RSC Adv.*, 2025, **15**, 3465.

30 A. Ciupa, *Anal. Methods*, 2025, **17**, 5782.

31 Selected examples: (*a*) P. Anastas and N. Eghbali, *Chem. Soc. Rev.*, 2010, **39**, 301; (*b*) R. A. Sheldon, *Chem. Soc. Rev.*, 2012, **41**, 1437; (*c*) R. A. Sheldon, *Chem. Commun.*, 2008, 3352.

32 Selected examples: (*a*) Z. Zhang, F.-W. Wang, S.-Q. Wang, F. Ge, B.-X. Zhao and J.-Y. Miao, *Org. Biomol. Chem.*, 2012, **10**, 8640; (*b*) Z. L. Gong, F. Ge and B.-X. Zhao, *Sens. Actuators, B*, 2011, **159**, 148; (*c*) M. M. Li, F. Wu, X. Y. Wang, T. T. Zhang, Y. Wu, Y. Xiao, J. Y. Miao and B.-X. Zhao, *Anal. Chim. Acta*, 2014, **826**, 77.

33 J. Vamathevan, D. Clark, P. Czodrowski, I. Dunham, E. Ferran, G. Lee, B. Li, A. Madabhushi, P. Shah, M. Spitzer and S. R. Zhao, *Nat. Rev. Drug Discovery*, 2019, **18**, 463.

34 A. Ciupa, *RSC Adv.*, 2025, **15**, 10565.

35 Selected examples: (*a*) D. C. Magri and A. A. Camilleri, *Chem. Commun.*, 2023, **59**, 4459; (*b*) D. Sammut, N. Bugeja, K. Szaciłowski and D. C. Magri, *New J. Chem.*, 2022, **46**, 15042; (*c*) N. Zerafa, M. Cini and D. C. Magri, *Mol. Syst. Des. Eng.*, 2021, **6**, 93.